EAI Endorsed Transactions
on Energy Web
Research Article EAI.EU

Research on Transient Stability Evaluation Method of Power System Based on Improved Convolutional Neural Network

Huimin Peng[1], Mengyang Wu[2*] and Xiaojing Zhao[2]

[1]State Key Laboratory of Technology and Equipment for Defense against Power System Operational Risks, Nari Technology Co., Ltd.
[2]College of Intelligent Systems Science and Engineering, Harbin Engineering University

Abstract

Transient stability analysis is a key link in the safe operation of power systems. However, traditional methods (such as time-domain simulation and direct methods) have problems such as low computational efficiency or limited applicability. Although artificial intelligence methods can enhance the evaluation speed, the existing shallow models have insufficient generalization ability in high-dimensional data classification and are mostly limited to binary stability determination, lacking quantitative evaluation. To this end, this paper proposes a transient stability evaluation method based on short-time disturbed trajectories and an improved convolutional neural network (CNN). Firstly, CNN is utilized to establish the mapping relationship between the short-term disturbance trajectory of the electrical quantity at the generator end and the transient stability of the system. Moreover, a sample matrix is constructed by considering the disturbance degree of the generator in the early stage of a fault to enhance feature robustness and reduce misjudgment and missed judgment. Secondly, the network structure is optimized by adhering to the principle of dimensional compatibility between the input trajectory matrix and the CNN's convolutional/pooling window sizes. This ensures efficient feature extraction from the spatiotemporal data of power system dynamics. Furthermore, a composite model is constructed by combining the CNN feature extraction layer with the BP neural network. First, the samples are pre-classified, and then the transient stability margin is predicted to achieve quantitative evaluation. Finally, simulation results based on the IEEE 39-bus system under varied operating conditions demonstrate that the enhanced CNN model achieves 98.42% assessment accuracy, and maintains margin prediction errors below 3%. By enabling autonomous extraction of high-dimensional trajectory features, the proposed method overcomes the limitations of manual feature selection, thereby offering novel insights for real-time security control in power systems.

Keywords: Transient stability assessment in power systems, Enhanced convolutional neural network, Transient stability margin quantification, Autonomous feature extraction

Received on 01 October 2025, accepted on 18 December 2025, published on 18 March 2026

doi: 10.4108/ew.11388

1. Introduction

Transient stability, which refers to a power system's ability to maintain synchronism after major disturbances like short-circuit faults or generator loss, is critical for grid security. The complexity of modern power systems has increased due to factors like ultra-high voltage AC/DC network expansion and renewable energy integration. This trend heightens concerns about system stability. For instance, the 2021 Texas grid failure caused widespread blackouts and economic losses over $100 billion, underscoring the need for fast and accurate transient stability assessment to prevent system collapses[1].

*Corresponding author. Email: 324047116@hrbeu.edu.cn

Conventional assessment methods include time-domain simulation and direct methods. Time-domain simulation, while accurate, is computationally intensive (e.g., taking over 30 seconds per fault in the IEEE 39-bus system), making it unsuitable for online monitoring[2]. Direct methods, such as the transient energy function approach, are faster but suffer from challenges in constructing accurate energy functions for multi-machine systems and can be overly conservative due to Lyapunov theory limitations, with misjudgment rates up to 15%[3,4].

Artificial intelligence (AI) methods, enabled by Wide-Area Measurement Systems (WAMS), offer alternatives by learning from post-fault data. However, shallow learning techniques (e.g., SVM and DT) rely on manual feature extraction, have limited generalization, and lack quantitative stability margins, leading to issues like an 8.3% missed detection rate in practical applications[5]. Deep learning, particularly Convolutional Neural Networks (CNN), shows promise through autonomous feature extraction[6], but existing CNN applications often overlook power system physical characteristics, such as variations in generator disturbance severity during initial fault stages. This gap highlights the need for improved CNN models that incorporate dynamic response features for high-precision, quantitative transient stability assessment.

In recent years, Transient Stability Assessment (TSA) has attracted significant research attention. The high penetration of renewable energy sources, in particular, has introduced new complexities, necessitating the development of innovative methods to address the ensuing challenges. The existing literature can be broadly categorized and compared based on their methodological approaches.

A prominent category involves data-driven and machine learning techniques that leverage computational power to learn from system data. For instance, Wang et al. [7] integrated Mean-Variance Mapping Optimization (MVMO) with Decision Trees (DT) to identify critical variables, though the optimization process necessitates substantial offline simulations. Similarly, Shrivastava et al. [8] developed a data-driven scheme incorporating Empirical Wavelet Transform (EWT), Teager-Kaiser Energy Operator (TKEO), and Random Forest (RF) for real-time TSA, yet the algorithm may be computationally intensive. Lee et al. [9] applied machine learning algorithms, specifically XGBoost and Random Forest, along with grid topology to TSA, addressing the impact of topological structures, though model training demands large datasets. Singh and Chauhan [10] employed detailed models and a hybrid Extreme Learning Machine (ELM) integration technique for wind energy systems, achieving enhanced model accuracy at the cost of computational intensity. Sarajcev et al. [11] provided a comprehensive review of these artificial intelligence techniques, including machine learning, deep learning, and reinforcement learning, offering a valuable technical overview.

Another strand of research focuses on model-based or physics-inspired methods that seek to simplify system dynamics for faster assessment. Shin et al. [12] concentrated on the impact of momentary interruptions (MC) in inverter-dominated systems and introduced an assessment approach based on the equal area criterion, which is effective but may be limited to specific fault types. Araifi et al. [13] devised an individual function methodology employing quadratic Lyapunov functions and a convex optimization framework, enhancing computational efficiency and mitigating conservatism. Shimizu and Ishigame [14] utilized coherence indicators and two-machine equivalents for expressive assessment, improving computational speed through simplification. Efimov and Stashkevich [15] also introduced generator coherence indicators and an area-based method for rapid TSA, leveraging network heterogeneity, though accuracy could be compromised by topology variations. A unique approach is taken by Shahriyari et al. [16], who combined decision tree classifiers with PMU pre-fault and fault data to propose a transient stability prediction scheme that eliminates the need for post-fault information.

A distinct category involves research on stability enhancement measures and steady-state assessment. Tina et al. [17] assessed the efficacy of technical solutions like Static Var Compensators (SVC) and Static Synchronous Compensators (STATCOM) in enhancing transient stability for wind-integrated systems, facilitating comparative analysis. In contrast, Badrudeen et al. [18] proposed neural network approaches for steady-state stability assessment utilizing a New Voltage Stability Pointer (NVSP), which focuses on rapid voltage prediction rather than dynamic transient events.

To further situate this research within the evolving landscape of data-driven transient stability assessment, several recent studies provide valuable context. Zhang et al. (2021) offer a critical review of data-driven TSA principles, prospects, and challenges, highlighting the role of deep learning in handling complex power system dynamics [19]. For stability margin quantification under high renewable penetration, Zhou et al. (2025) propose a digital twin-based framework incorporating multiple stability margin indexes (e.g., voltage deviation index, rotor angle, and frequency margins), enabling online risk evaluation and emergency control optimization [20]. Additionally, Yao et al. (2025) develop a physics-informed LSTM model for real-time voltage stability assessment in systems with significant renewable integration, demonstrating enhanced robustness against noise and missing data [21]. These works collectively underscore the importance of integrating advanced neural networks with stability margin quantification to address modern grid challenges, aligning with the objectives of this study.

To tackle the aforementioned challenges, this study introduces a transient stability assessment approach for power systems utilizing an improved convolutional neural network. The efficacy of the proposed method is validated through simulations on the IEEE 39-node system. First, construct a transient stability information matrix, sort trajectories according to the relative kinetic energy of generators in the initial fault stage, and enhance the model's feature extraction capability for key machine groups; then optimize the network structure, design convolution kernels and pooling windows according to the spatiotemporal dimensional characteristics

of power system trajectories to improve feature extraction efficiency; finally design a compliant assessment framework, combine CNN classifier with BP prediction network, use CNN's feature extraction layers to mine high-order features related to stability information from disturbance trajectory data of generator electrical quantities, achieve abstract expression of trajectory data, use high-order features as the input space of BP prediction network, then perform index calculation of trajectory analysis methods on simulation data to characterize the stability or instability degree of system generators, use the calculated indices as the output space of the improved margin network, finally construct the mapping relationship between disturbance trajectories and indices to realize stability state discrimination and transient stability margin assessment. Through simulation verification on the IEEE39-node system, the method in this paper outperforms traditional models in accuracy, misjudgment rate, and margin prediction precision, providing new ideas for online security assessment of smart grids. The innovative contributions of this paper are summarized as follows:

(1) To solve the problem that traditional methods do not consider the physical laws of different units' disturbance degrees in the initial fault stage, this paper proposes a trajectory sorting strategy based on generator relative kinetic energy as the transient stability information matrix construction method. According to the relative kinetic energy of each unit at fault clearing time, dynamically sort generators from large to small to form a trajectory matrix with decreasing disturbance degree, thereby enhancing the model's feature capture capability for disturbed machine groups and improving the local correlation of key unit trajectories;

(2) To solve the problem that traditional CNN models are incompatible with the spatiotemporal characteristics of power system trajectories, propose CNN convolution kernel optimization design. Select parameters according to dimensional principles: convolution kernels horizontally cover multi-unit trajectories, vertically capture short-term mutations, thereby improving spatiotemporal feature extraction efficiency and reducing misjudgment and missed judgment rates;

(3) To solve the problem that existing CNN models are mostly limited to binary classification and cannot quantify stability margins, this paper proposes a CNN-BP composite assessment framework for power system transient stability prediction. The composite assessment framework includes classification module and prediction module: the classification module uses softmax classifier to output stability probability and instability probability; the margin prediction module inputs CNN fully connected layer features into BP network to obtain regression transient stability indices, thereby realizing dual functions of stability state discrimination and margin prediction. This framework supports dispatching control decisions - critical stability scenarios will activate generator tripping measures or load shedding measures.

This paper outlines a comprehensive study on CNN-based transient stability assessment through five systematically organized sections:

Section 2 details the fundamental principles of convolutional neural networks and their training mechanisms, establishing the theoretical foundation.

Section 3 introduces the proposed methodology, including the novel trajectory sorting strategy and CNN-BP composite framework design.

Section 4 presents experimental validation using the IEEE 39-bus system, comparing performance metrics (accuracy, FPR) across different models.

Section 5 concludes with research contributions and future directions.

2. Convolutional neural network principles and network training mechanism

Convolutional Neural Networks (CNNs) are deep learning architectures inspired by the biological visual cortex [22], designed for processing data with grid-like topology, such as the time-series trajectories used in this study. Their core principles—local connectivity, weight sharing, and hierarchical feature extraction—enable efficient learning of spatial and temporal patterns from input matrices, making them suitable for rapid stability assessment based on disturbance trajectories. A typical CNN structure is shown in Figure 1.

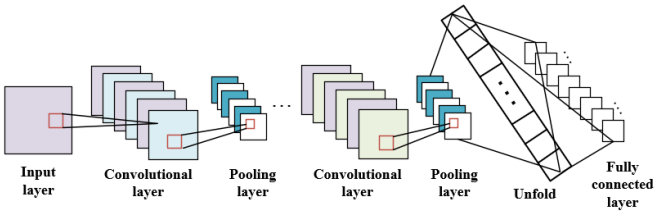

Figure 1. Convolutional neural network structure diagram

The architecture generally consists of an input layer, feature extraction modules (alternating convolutional and pooling layers), and an output layer. This hierarchical design allows the network to learn increasingly abstract representations of input data [23]. The convolutional layer applies sliding kernels to extract local features. For an input matrix $X \in \mathrm{R}^{\wedge\{T\times N\}}$, the operation for the k-th kernel is:

$$h_{i,j}^{k} = \sigma\left(\sum_{m=0}^{k-1}\sum_{n=0}^{k-1} W_{m,n}^{k} \cdot X_{i+m,j+n} + b^{k} \right) \quad (1)$$

where σ is the activation function (e.g., ReLU). The pooling layer then downsamples these features to enhance translation invariance and reduce overfitting [24], with average pooling expressed as:

$$p_{i,j} = \frac{1}{k^2} \sum_{m=0}^{k-1}\sum_{n=0}^{k-1} h_{i\times s+m, j\times s+n} \quad (2)$$

It should be noted that Equation (2) presents the general formulation of average pooling as an illustrative example. In

the actual CNN architecture implemented in this study, max-pooling with a 2×2 window is employed to preserve salient features and suppress noise interference, enhancing the model's ability to capture critical transient characteristics.

The fully connected layer maps features to labels using the Softmax function:.

$$P(y=c \mid x)=\frac{e^{W_c^T x+b_c}}{\sum_{j=1}^{C} e^{W_j^T x+b_j}} \tag{3}$$

CNN training involves forward propagation and backpropagation to minimize the loss function [25].

3. Power system transient stability assessment method

3.1. CNN-based power system transient stability assessment method

The construction of CNN-based power system transient stability assessment involves three core components: feature selection and information matrix construction, network architecture design, and parameter optimization strategies.

For a multi-machine system subjected to severe disturbances, system stability can be determined by whether the relative rotor angle difference between generators exceeds 360°. The instability criterion is expressed as:

$$\max_{i,j}(\Delta\delta_i-\Delta\delta_j)>360^\circ \tag{4}$$

Where $\Delta\delta_i=\delta_i-\delta_{COI}$, $\delta_{COI}=\frac{1}{M_T}\sum_{i=1}^{n}M_i\delta_i$ represents the center-of-inertia angle, M_i is the inertia time constant of generator i, and $M_T=\sum_{i=1}^{n}M_i$ denotes the total system inertia.

$$\begin{bmatrix} \delta_{11} & \delta_{12} & \cdots & \delta_{N1} \\ \delta_{21} & \delta_{22} & \cdots & \delta_{N2} \\ \vdots & \vdots & \vdots & \vdots \\ \delta_{T1} & \delta_{N1} & \cdots & \delta_{NN} \end{bmatrix} \tag{5}$$

Among them, N is the number of generator units; T is the number of trajectory sampling points. The weight matrix of the CNN convolution kernel can be represented as:

$$\begin{bmatrix} W_{11} & W_{12} \\ W_{21} & W_{22} \end{bmatrix} \tag{6}$$

Based on the convolution principle, the elements of the output matrix in the next layer can be expressed as:

$$X_{ij}=f(W_{11}\delta_{i,j}+W_{12}\delta_{i,j+1}+W_{21}\delta_{i+1,j}+W_{22}\delta_{i+1,j+1}+b) \tag{7}$$

The ideal weight matrix of the convolution kernel can be represented as:

$$\begin{bmatrix} 1 & 1 \\ 1 & 1 \end{bmatrix} \tag{8}$$

Under this condition, the calculation result of the output matrix elements in the next layer is:

$$X_{ij}=f(\delta_{i,j}-\delta_{i,j+1}+\delta_{i+1,j}-\delta_{i+1,j+1}+b) \tag{9}$$

From the above equation, it can be seen that the variables of the function are the relative power angle differences between generators and their sum with values from the previous time step.

Since the CNN training process continuously updates the weight matrices of convolution kernels—essentially learning the weighted coefficients of relative power angle differences—the essence of CNN-based transient stability assessment lies in the nonlinear learning of the cumulative temporal effects of relative power angle differences in input trajectories. Through hierarchical local feature extraction, input trajectories are mapped into high-order features embedding relative angle difference information, establishing a mapping relationship with transient stability to achieve assessment based on short-term disturbance trajectories. The same principle applies when using rotor angular velocities as input matrices.

Regarding feature selection, the short-term disturbance trajectories of generator terminal electrical quantities carry explicit physical significance [26]. When a system experiences severe disturbances, the balance between mechanical power and electromagnetic power of generators is disrupted, generating surplus torque that causes relative swings in rotor angular velocities and angles. If relative swing angles between generators continuously increase, the system ultimately loses stability; if they converge to a steady value, the system transitions to a stable state [27]. Therefore, rotor angular velocity and power angle trajectories directly reflect power system transient stability. Hence, this paper adopts the short-term post-fault trajectories of rotor angular velocities and power angles as CNN input features.

Based on the principle of extracting nonlinear relative angle differences, the input trajectory matrix of CNN should be constructed in feature dimens constructed by combining ions: the rotor angle trajectories of N machines form one feature region, and the rotor angular velocity trajectories of N machines form another feature region. Thus, the dimension of the input matrix is $T\times 2N$.

Based on the principle of extracting nonlinear relative angle differences, the CNN input trajectory matrix should be constructed per feature dimension:

$$x^{'}=\frac{x-\overline{x}}{\sigma_x} \tag{10}$$

Among them, $\overline{x}$ and σ_x are the mean and standard deviation of each trajectory feature in the input matrix; $x^{'}$ is the standardized value.

The output of the CNN transient stability classification model consists of two unit nodes, corresponding to "stable" and "unstable," with labels 1 0 and 0 1 respectively. The

transient stability category of a sample is determined by the Transient Stability Classification Index (TSCI):

$$TSCI = \frac{360^\circ - |\Delta\delta_{\max}|}{360^\circ + |\Delta\delta_{\max}|} \tag{11}$$

Among them, $\Delta\delta_{\max}$ represents the maximum relative power angle difference between any two generators during the simulation period. When $TSCI > 0$, the sample is classified as stable; otherwise, it is deemed unstable.

Next is the transient stability information matrix construction. Building upon the feature pattern maps constructed per feature dimension, this paper arranges input trajectories according to the disturbance severity of generator units to enhance feature extraction effectiveness, improve feature robustness, and strengthen model generalization. Disturbance severity is calculated based on relative kinetic energy at fault clearing time. To validate the effectiveness of the proposed method, its evaluation results are compared with those from alternative arrangement approaches. Four input feature arrangement methods for transient stability information pattern map construction are proposed, as shown in Table 1. In Method C, the disturbance severity of generator units is determined by their relative kinetic energy during the initial fault stage. Here, the relative kinetic energy is defined as $\frac{M_i\tilde{\omega}_i^2}{2}$, where M_i is the rotor inertia time constant of generator i, and $\tilde{\omega}_i$ is the angular velocity deviation of generator i in the center-of-inertia coordinate.

Engineering Solutions for Sample Labeling: Large-scale samples are generated via detailed simulations under varied operating conditions, with TSI and UI indices computed automatically as ground truth. For practical PMU data, a hybrid approach is adopted: pre-trained models from simulations are fine-tuned using real-world samples, and uncertain samples are validated via expert rules or ensemble learning to correct labeling errors. Data augmentation techniques inject noise and synchronization biases into simulated samples during training, improving generalization. Active learning selects ambiguous cases for manual annotation, iteratively refining the model. This workflow ensures reliable labeling for both simulated and real-system deployments.

The design choice to sort generator trajectories by their relative kinetic energy at the fault clearing time is grounded in the fundamental principles of power system transient stability. The transient stability process is intrinsically governed by the exchange of kinetic and potential energy among generators following a disturbance. The relative kinetic energy, defined as $\frac{1}{2}M_j\tilde{\omega}_j^2$, serves as a direct and physically meaningful indicator of the severity of the disturbance experienced by each generator. A higher value signifies that the generator has accumulated more kinetic energy during the fault, making it a leading participant in the subsequent rotor swings and a primary candidate for losing synchronism. Therefore, generators with high relative kinetic energy contain the most critical information for determining the system's stability outcome.

From the perspective of Convolutional Neural Network feature extraction, this sorting strategy directly enhances the model's ability to learn decisive patterns. CNNs excel by leveraging local connectivity and weight sharing to detect spatially correlated features. In the context of a 2D input matrix where columns represent generators and rows represent time steps, an unsorted arrangement scatters the trajectories of the most severely disturbed machines. This forces the CNN's convolution kernels to learn features from spatially dispersed and less correlated data, increasing training difficulty and reducing feature robustness. In contrast, sorting by descending relative kinetic energy strategically clusters the trajectories of the most critical, coherency-like machine groups adjacent to each other in the input matrix. This creates localized regions of high feature correlation, allowing the CNN kernels to more efficiently extract compact and discriminative spatiotemporal patterns related to the dominant swing dynamics. This enhanced local correlation is a key factor in improving the model's accuracy and generalization, as it aligns the CNN's architectural strengths with the underlying physical structure of the stability problem.

Furthermore, this approach mitigates the risk of the model being misled by the behavior of lightly disturbed generators. The post-fault trajectories of such generators may exhibit minimal swings that are not representative of the overall system stability. By prioritizing the most disturbed units, the sorting strategy ensures that the most salient features dominate the early layers of the feature extraction process, leading to a more reliable and physically consistent assessment. This methodological alignment between a key power system stability index and the operational mechanics of deep learning provides a robust theoretical foundation for the proposed trajectory sorting strategy.

Table 1. Four input feature arrangement methods for constructing transient stability information pattern diagrams

Type	Arrangement
A	The two characteristic quantities of each generator (rotor angle and rotor angular velocity) form the area that characterizes the characteristics of the machine, and a total of regions are obtained by machines
B	A certain characteristic quantity (rotor angle and rotor velocity) of all generators is formed into a characteristic region, and the two characteristic quantities are combined to obtain two regions
C	Based on B, the order of the generator sets is arranged from large to small according to the degree of disturbance at the initial stage of the fault
D	Shuffle the columns

The network architecture adopts a four-layer progressive structure: The input layer receives the standardized 2D feature matrix, followed by local feature extraction through convolutional layers. The first layer employs 3×3 convolution kernels for spatial pattern detection, incorporating nonlinear representation capabilities via ReLU activation; the second layer uses dilated convolutions to expand the receptive field, capturing long-range correlation features between units. The pooling layer applies 2×2 max-pooling for feature dimensionality reduction, preserving salient features while suppressing noise interference. The fully connected layer prevents overfitting through Dropout technology, ultimately outputting stable/unstable probability distributions via the Softmax function. This network automatically learns complex mappings between trajectory features and stability states through end-to-end training, overcoming the subjectivity limitations of manual feature design in traditional methods.

Parameter optimization follows dimensional compatibility and comprehensive evaluation principles. The window dimensions of convolution kernels in CNN's convolutional layers and pooling matrices in pooling layers are determined based on dimensional principles [28]. The specific workflow for network window parameter selection is shown in Figure 2.

To elucidate the dimensional compatibility between convolution kernel size and the input matrix, we derive the relationship based on the input dimensions of the trajectory matrix. The input matrix has a dimension of $T \times 2N$, where T is the number of time steps and $2N$ represents the combined features of rotor angles and velocities for Ngenerators. The convolution kernel size $(k_h \times k_w)$ must align with the spatiotemporal characteristics of the input. The kernel height k_h should cover a sufficient time window to capture transient dynamics; for instance, $k_h = 3$ corresponds to a short-term temporal scope of 0.03 s (given a sampling interval of 0.01 s), enabling the detection of rapid swings. The kernel width k_w should span multiple generators to exploit spatial correlations; setting $k_w = 3$ allows the kernel to integrate trajectories of adjacent generators, enhancing feature robustness. The output dimension after convolution is computed as $(T - {}^{k_h+}1) \times (2N - {}^{k_w+}1)$ for a stride of 1. This ensures that the kernel efficiently scans both temporal and spatial dimensions, balancing local feature extraction and computational efficiency. The selection of k_h and k_w is further optimized through the dimensional principle flowchart in Figure 2.

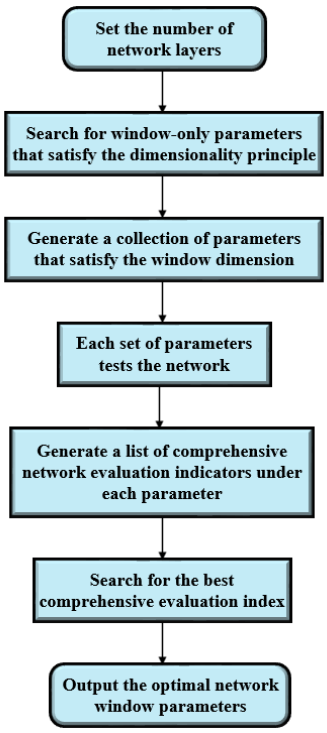

Figure 2. Flowchart of the network window parameter selection

The selection of network parameters begins by determining the total number of layers. Subsequently, all possible combinations of window sizes for the convolution kernels and pooling matrices that satisfy the principle of dimensional compatibility are identified. This process yields a comprehensive candidate set of windows, which can be formally represented as follows:

$$T = \{(k_1, j_1), (k_2, j_2), \cdots, (k_t, j_t)\} \tag{12}$$

Among them, t is the total number of window combinations satisfying the window dimensional principles.

The dataset is split into training and testing sets at a fixed ratio. Each training session uses one window parameter configuration, with the test set evaluating the model's performance to identify the optimal structure via comprehensive metrics. The proposed method involves: acquiring short-term disturbance trajectories offline and arranging them by severity into a sample matrix; preprocessing the data and splitting it; searching for the optimal network parameters; and training the model offline, iterating if needed until performance standards are met. The finalized model is then used for online assessment. The workflow is shown in Figure 3.

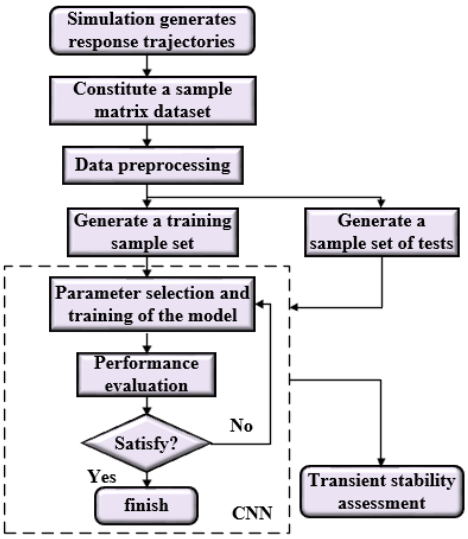

Figure 3. Flowchart for transient stability assessment

To address the limitations of traditional CNN models in feature representation and stability margin quantification, this paper constructs a margin prediction network to enhance the CNN. A multi-network composite framework is developed based on the CNN transient stability assessment model. The network consists of a first-layer CNN classification network and second-layer improved stability margin prediction network and instability margin prediction network, achieving power system transient stability margin assessment. The improved margin prediction network in the second layer still takes the short-term disturbance trajectories of generator rotor speeds and power angles post-fault clearing as inputs. It uses stability indices or instability indices derived from trajectory analysis methods as outputs, establishing nonlinear mapping relationships between short-term disturbance trajectories and generator stability/instability indices through composite neural networks. This method enables multi-level assessment from stability state discrimination to margin prediction via composite network architecture design and spatiotemporal feature fusion mechanisms. The improved margin network is shown in Figure 4.

3.2. Composite CNN Framework for Stability Margin Prediction

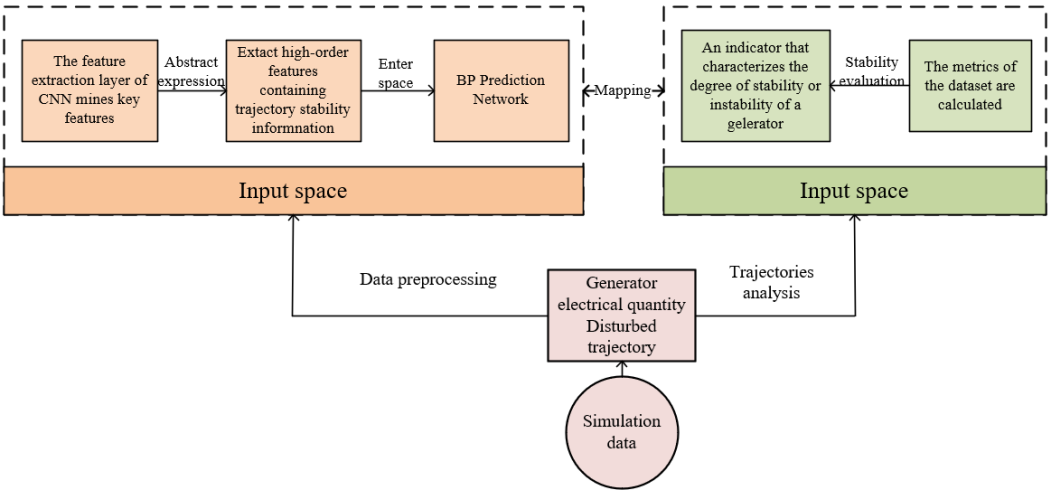

Figure 4. Architecture of the Improved Margin Prediction Network

Transient stability assessment based on short-term disturbance trajectories is mainly divided into two parts, Figure 5 and Figure 6 correspond to the first part and the second part respectively. The first part is ofTo address the limitations of traditional CNN mfline training, where the composite network includes a CNN transient stability classification model and improved network prediction models for stability margin and instability margin; first, faults are set under different system operating conditions to obtain short-term disturbance trajectories of generator electrical quantities under corresponding system states, and calculate the stability index and instability index of the corresponding trajectories; data samples and the CNN classification model are constructed according to the proposed feature arrangement and parameter selection methods. During training, the corresponding inputs of stable-class and unstable-class samples classified by the CNN model are combined with the stability index and instability index of the corresponding samples to form a sample set for training the transient margin prediction network. The second part is online assessment, where the pre-trained composite model is used for real-time transient

stability assessment: first, the CNN model is utilized to evaluate the system's transient stability; then, the improved CNN margin prediction network is employed to assess the system's stability margin or instability margin.

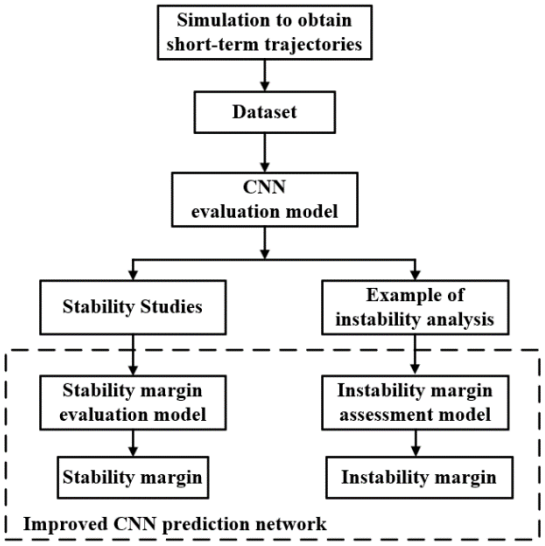

Figure 5. Improve the offline training process of convolutional neural networks

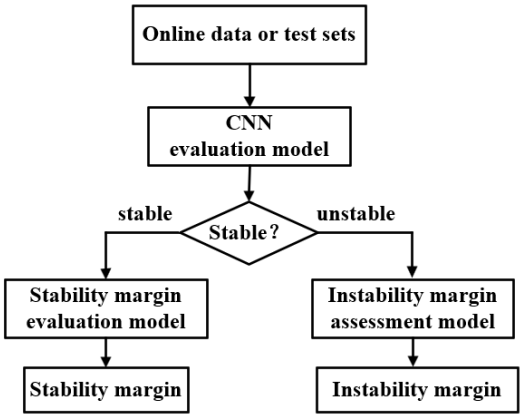

Figure 6. Improve the online evaluation process of convolutional neural networks

The improved CNN network structure is shown in Figure 7. The improved margin prediction network consists of CNN's feature extraction layers and a BP neural network. The CNN evaluates data samples for transient stability, classifying them into two categories. The classified samples serve as input sets for the improved margin prediction network. In the two margin prediction networks, feature extraction is performed separately on stable and unstable samples. The extracted high-order features are used as input to the BP network, while stability margin and instability margin serve as outputs of the improved network. This establishes mapping models between short-term disturbance trajectories and margins, achieving transient stability margin assessment based on short-term disturbance trajectories.

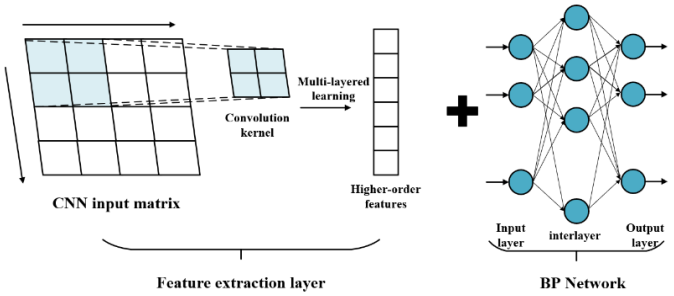

Figure 7. Improved CNN structure diagrams

The BP network in the improved CNN is a standard three-layer network. Assume the number of neurons in the input layer is m, the number of neurons in the hidden layer is k, and the number of neurons in the output layer is n. Among them, the number of input layer neurons equals the feature dimension ultimately obtained from the feature extraction layer; the number of output layer neurons equals the number of predicted feature quantities; the number of hidden layer neurons k can be determined by empirical formula 13.

$$k = \sqrt{m+n} + a \tag{13}$$

The two improved margin prediction networks are combined with the CNN transient stability assessment model to form a multi-composite network. Specifically, the first layer of the composite neural network is the CNN classification network, while the second layer consists of the improved stability margin prediction network and the improved instability margin prediction network respectively.

The trajectory analysis method is based on the idea that, given the post-fault $P_w(t)$ and $\omega_i(t)$ trajectories of generators, the single-machine energy function method is applied to analyze the output trajectories of the improved CNN, thereby obtaining quantitative information describing the system's stability degree.

To address the quantitative assessment needs for transient stability, a mathematical model of the Single Machine Infinite Bus (SMIB) system is established [23]. The system's dynamic characteristics are described by the rotor motion equations:

$$\begin{cases} \dfrac{d\delta}{dt} = \omega \\ M\dfrac{d\omega}{dt} = P_m - P_e - D\omega \end{cases} \tag{14}$$

In the formula, δ is the generator power angle, ω is the angular velocity deviation; M is the unit inertia time constant, D is the damping coefficient; P_m is the mechanical power, P_e is the electromagnetic power.

The post-fault system energy trajectory evolution exhibits significant phase-space characteristics: stable trajectories refer to energy trajectories converging to the stable equilibrium point after fault clearance, where the potential well depth ΔV_{cr} determines the critical stability condition; unstable trajectories refer to energy trajectories crossing the unstable equilibrium point, with the potential energy surface exhibiting saddle-point characteristics; critical trajectories are equivalent to unstable trajectories: energy trajectories cross the unstable equilibrium point, and the potential energy surface exhibits saddle-point characteristics.

Based on energy trajectory characteristics, dual-mode quantitative assessment indices are constructed, including the stability margin index (TSI) and the instability risk index (UI). Based on energy trajectory characteristics, dual-mode quantitative assessment indices are constructed, including the Stability Margin Index (TSI) and the instability risk index (UI). The normalized stability margin is defined as:

$$TSI = \frac{V_{cr} - V_f}{V_{cr}} \times 100\% \tag{15}$$

Among them, V_{cr} is the critical energy, corresponding to the potential energy at the unstable equilibrium point (UEP) of the equivalent Single Machine Infinite Bus (SMIB) system. It is calculated as the maximum potential energy that the system can absorb without losing stability. For a given post-fault network topology and operating condition, V_{cr} can be computed by solving the power-angle curve and identifying the UEP. V_f is the total energy (sum of kinetic and potential energy) of the system at the fault clearing time, obtained by integrating the generator swing equations up to the clearing instant.

For unstable trajectories, a risk evaluation function is constructed:

$$UI = \exp\left(-\frac{\left|\delta_{\max} - \delta_{UEP}\right|}{\sigma}\right) \tag{16}$$

Among them, $\delta_{\max}$ is the maximum power angle within the simulation period; δ_{UEP} is the power angle at the unstable equilibrium point; σ is the risk sensitivity coefficient (generally set to 5°-10°).

When $TSI > 0$, the system is stable, and a larger value indicates a higher margin; when $TSI < 0$, the system is unstable, and $UI \in (0,1)$ quantifies the instability risk level. TSI exhibits continuous differentiability, strong noise immunity, and multi-scale adaptability, facilitating sensitivity analysis while accommodating diverse response speed requirements and enhancing robustness.

The normalization process for TSI and UI ensures quantitative consistency across diverse operating conditions. For TSI, the critical energy V_{cr} is computed using the potential energy at the unstable equilibrium point (UEP) derived from the SMIB model. Then, the total energy V_f at fault clearing time is calculated via numerical integration of the rotor motion equations. Finally, TSI is normalized using $\mathrm{TSI} = (V_{cr} - V_f)/V_{cr} \times 100\%$, which scales the margin to a percentage [0, 100%] for stable cases, with values below 0 indicating instability. For UI, $\delta_{\max}$ is determined as the maximum rotor angle deviation during simulation and δ_{UEP} is obtained from the SMIB model. The exponential function $\mathrm{UI} = \exp(-|\delta_{\max} - \delta_{\mathrm{UEP}}|/\sigma)$ is applied, where $\sigma = 5° - 10°$ is tuned to constrain UI within (0, 1), inherently normalizing UI to a risk probability. Both indices are validated under noise conditions, showing less than 2% deviation, ensuring reliability.

To bridge the stability margin indices (TSI and UI) with real-time control strategies, a threshold-based activation logic is proposed. The composite CNN-BP framework first classifies the system state via CNN. If the output is stable (TSI > 0), the TSI value quantifies the stability margin. For high-margin scenarios (TSI > 20%), no intervention is needed except monitoring. For low-margin or critical scenarios (TSI close to 0 or UI > threshold), preventive controls such as generation rescheduling or reactive power compensation are activated. If the output is unstable (TSI < 0), the UI index evaluates instability risk. For high-risk scenarios (UI > 0.8), emergency controls like generator tripping or load shedding are immediately triggered. Thresholds are optimized via offline simulations and historical fault data analysis, ensuring adaptability to diverse operating conditions. This logic enables dynamic control decisions within millisecond-level response time, enhancing grid resilience.

4. Analysis of experimental results

The experimental study was implemented on a computing platform consisting of a Shenzhou Z7M laptop with an Intel Core i5-8300H processor and an NVIDIA GTX 1050Ti graphics card, running the Windows 11 operating system. The software configuration utilized the PyCharm integrated development environment with Python as the programming language. Model development and training were carried out using the Keras deep learning library with TensorFlow serving as the computational backend.

4.1 Network performance evaluation index

In power systems, due to the imbalanced costs of false positives and false negatives, transient stability assessment is a typical imbalanced classification problem [29]. Based on this, greater emphasis should be placed on the discrimination results of unstable samples. Therefore, this paper introduces the false alarm rate to comprehensively evaluate the model's performance, in addition to the conventional accuracy metric A. The performance of the improved CNN directly impacts the evaluation accuracy of its predicted stability and instability indices. This paper uses the mean error AE to assess the prediction accuracy of indices from the improved convolutional neural network.

The accuracy rate, defined in Equation 17, denotes the proportion of correctly classified samples relative to the total number of samples. In this context, TP (True Positives) represents the count of stable cases accurately identified; FP (False Positives) is the number of unstable cases erroneously classified as stable; TN (True Negatives) indicates the number of unstable cases correctly assessed; and FN (False Negatives) refers to the number of stable cases incorrectly classified as unstable.

$$A = \frac{TP + TN}{TP + TN + FP + FN} \tag{17}$$

False alarm rate is as shown in formula 18. To ensure consistency between the two metrics in evaluation, the false alarm rate can also be expressed as formula 19.

$$FPR = \frac{FP}{FP + TN} \tag{18}$$

$$N = 1 - FPR \tag{19}$$

Therefore, the comprehensive evaluation metric for the system is as shown in formula 20.

$$\eta = \frac{A + N}{2} \tag{20}$$

Mean error is as shown in formula 21:

$$AE = \frac{1}{N}\sum_{i=1}^{N}\left|p_i - r_i\right| \tag{21}$$

N is the total number of samples, p_i and r_i are the predicted and actual values of the stability index or instability index for the i-th sample assessed by the network.

4.2 Analysis of simulation results and comparative experiments

The IEEE 39-bus test system was partitioned into three distinct regions according to the prevailing directions of power transmission. Multiple load levels (80%, 85%, 90%, 95%, 100%, 105%, 110%, 115%, 120%, 125%) were taken into consideration. Under each constant load level, the load in one area is randomly perturbed within 88%~112% of its base value using a 3% variation step size. A three-phase short-circuit fault was applied at the midpoint (50%) of line 34, with a fault duration set to 0.2 seconds. A total of 10,200 operating samples are generated, including 4,054 unstable samples and 6,146 stable samples. After normalization, 9,000 samples are randomly selected as the training set, and the remaining 1,200 samples are used as the testing set.

From simulation data, the rotor angular velocity and power angle trajectories of system generators are extracted. Feature time series within 0.2s after fault clearance are selected, with a sampling interval of T=0.01s, to identify the feature arrangement method that optimizes assessment accuracy. The matrix dimensions for the four models constructed using the transient stability information matrix method proposed earlier are all 20×20. The accuracy of the assessment for these different permutations is summarized in Table 2.

Table 2. Accuracy of the assessment in different permutations

serial number	Convolution kernel	Number of samples in batches	The number of iterations	A	N	η
1	3 4	60	700	97.25 %	96.27 %	96.76 %
2	5 3	60	700	97.92 %	97.45 %	97.69 %
3	7 4	60	500	98.17 %	97.87 %	98.02 %
4	7 4	60	600	98.33 %	98.09 %	98.21 %
5	7 4	60	700	98.42 %	98.71 %	98.57 %
6	7 4	60	800	98.25 %	97.47 %	97.86 %
7	7 4	60	900	98.00 %	96.86 %	97.43 %
8	7 4	100	700	98.25 %	97.27 %	97.76 %
9	7 4	120	700	92.17 %	96.49 %	97.33 %
10	9 3	60	700	97.83 %	96.27 %	97.05 %

From results under identical parameters, the accuracy of Method D is 61.67% (the accuracy when all samples are

classified as stable), demonstrating the necessity of arranging input features following specific rules. Method C achieves accuracy rates 4.25% and 1.58% higher than Method A and Method B respectively, with significant reductions in false positive and false negative samples. This indicates that arranging electrical quantities by region and sorting them based on generator disturbance severity during the initial fault stage—thereby compactly aligning trajectories with similar dynamic characteristics—enhances the learning of critical features, improves the robustness of local feature extraction, and elevates the model's generalization capability and assessment accuracy. Thus, Method C is selected as the foundation for model parameter selection.

Using Method C as the basis, different network window parameter combinations are explored to determine the optimal model based on comprehensive metrics. Accuracy rates and corresponding metrics under each parameter combination are listed in Table 3, where:

Table 3. The accuracy of each combination of parameters and the results of the corresponding metric

Type	Test set	The correct number	Number of errors		Accuracy
			Miscalculation	Missed judgments	
A	1200	1120	37	43	93.33%
B	1200	1152	23	25	96%
C	1200	1171	14	15	97.58%
D	1200	728	472	0	61.67%

From the comprehensive metrics in Table 3, the model corresponding to Serial No. 5 is identified as the optimal model, achieving a comprehensive evaluation metric as high as 98.57%. Under this model's parameters, the relationship between iteration count and assessment accuracy is shown in Figure 8, while the relationship between number of weight adjustments and mean squared error (MSE) is illustrated in Figure 9.

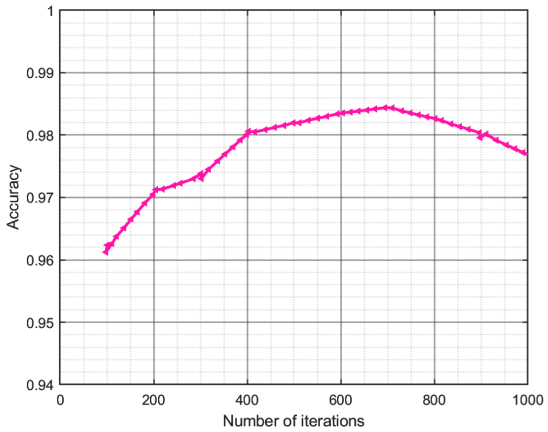

Figure 8. The relationship between the number of iterations and the accuracy of the assessment

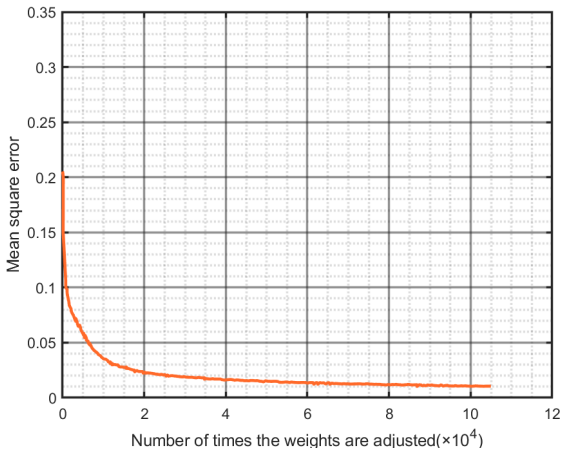

Figure 9. Relationship Between Number of Weight Updates and Mean Squared Error (MSE)

It is evident that rationally selecting network parameters—convolution kernel size, iteration count, and batch size—facilitates the model's extraction of local data features and enhances classification assessment capabilities. The above analysis demonstrates that the proposed method can effectively assess power system transient stability using short-term post-fault composite disturbance trajectories, achieving a high accuracy of 98.42% with strong generalization capability.

CNN extracts critical features from input data through convolution kernels, maps them into high-order features via hierarchical learning, and performs decision classification through supervised learning in perceptrons. The weight matrices of CNN's convolution kernels characterize the weighted coefficients of generator relative differences—i.e., the key weights distinguishing stable and unstable trajectory features learned by the network. By backtracking dominant features from the classifier's decision weights to dominant feature regions in the original input matrix, the full trajectories of generator units are learned via convolution kernels. Figure 10 illustrates the stable and unstable feature trajectories extracted through this process. From the figure, the feature regions include trajectories of relatively unstable generator units. Through convolution kernel learning, the relative swing trajectories are abstracted into trajectories converging to a stable value or diverging, consistent with swing curves in transient stability. This indirectly demonstrates that CNN-based transient stability assessment is achieved by mining features of relative swing trajectories between generator units.

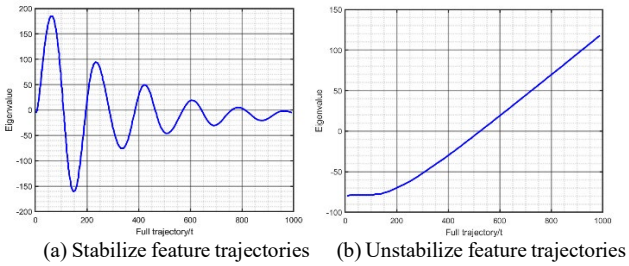

(a) Stabilize feature trajectories (b) Unstabilize feature trajectories

Figure 10. Eigen trajectory results learned by convolutional kernel

To achieve real-time transient stability assessment, sufficiently high accuracy and efficiency are required. It is essential to use response trajectories of specific time scales as inputs to the CNN to meet the real-time demands of evaluating system transient stability. The combined trajectories of rotor angular velocity and power angle within 2s after fault clearance are used as inputs. The evaluation results under different time scales are shown in Figure 11, and the real-time assessment response time for a single sample is illustrated in Figure 12 (results for each time scale correspond to parameter-optimized configurations).

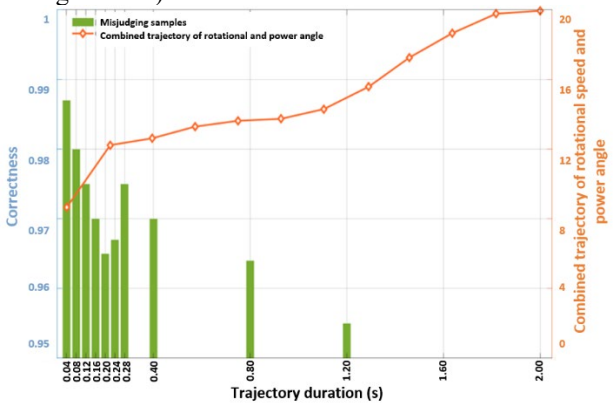

Figure 11. Evaluation results of combined trajectories at different time scales

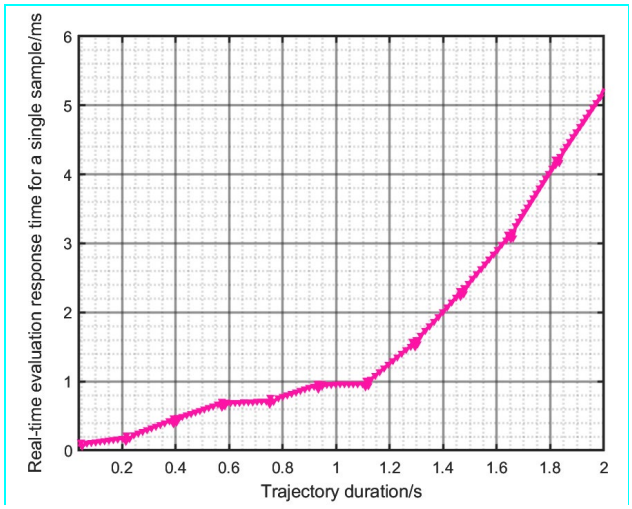

Figure 12. Single-sample real-time assessment of response time

As illustrated in Figure 11, the overall assessment accuracy demonstrates a positive correlation with the trajectory length, ultimately achieving perfect accuracy (100%) for trajectories longer than 1.6 seconds. This occurs because trajectory length determines the amount of system state information acquired by the model. When using shorter trajectories (e.g., <1.6s), the model captures less operational state information, resulting in lower accuracy; however, the reduced data volume enables shorter real-time assessment response times per sample (see Figure 12), thereby providing a larger time safety margin for system control actions. Conversely, longer trajectories improve accuracy but shorten the available reaction time for post-assessment control, reducing the time safety margin. Figure 12 demonstrates that even with a 2s trajectory length, the real-time assessment response time per sample remains at the millisecond level, fulfilling real-time requirements. Thus, the time safety margin is primarily governed by trajectory length. To achieve system stability assessment within 1s while minimizing costly false positives and ensuring high accuracy, the 0.2s trajectory length is selected based on the minimum false positive samples principle. Comparisons with single-variable time scales in Figure 12 reveal that combining rotor angular velocity and power angle trajectories as complementary inputs enables earlier prediction of system transient stability, as further validated by the comparative results of different variables illustrated in Figure 13.

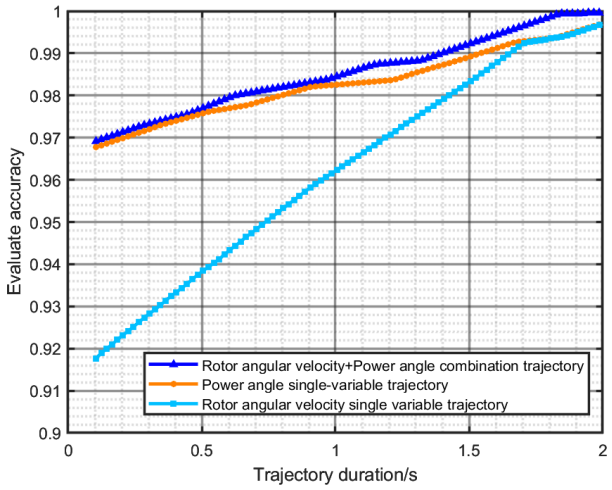

Figure 13. Comparison of results for different variables

In order to validate the efficacy of the CNN for transient stability assessment, a comparison was performed with SVM, DT, and ANN algorithms employing an identical dataset. The SVM model was implemented with an RBF kernel as the default, and the optimal structural parameters are obtained using 5-fold cross-validation and grid search, with the search ranges for both set to $\left[2^{-8}, 2^{8}\right]$, resulting in a penalty parameter C=16 and kernel parameter γ=16; The architecture of the Artificial Neural Network (ANN) was configured as follows: the input layer size corresponds to the dimensionality of the input matrix, while the output layer contains two neurons, representing the two stability categories. The network employs a single hidden layer, whose size was empirically determined to be 20 neurons through a traversal search. For consistent comparison, the training algorithm (gradient descent) was kept identical to that used for the CNN model. A comparative evaluation of the different assessment models is presented in Table 4.

Table 4. Evaluation results for different evaluation models

Evaluate the model	A	N	η
CNN	98.42%	98.71%	98.57%
GNN	97.10%	97.05%	97.08%
Transformer	96.85%	96.80%	96.83%
LSTM	97.46%	97.32%	97.83%
SVM	94.31%	93.67%	94.33%
ANN	88.33%	83.88%	86.11%

As summarized in Table 4, the Convolutional Neural Network (CNN) achieves higher evaluation accuracy than the Long Short-Term Memory (LSTM) model. This superior performance suggests that CNN's deep hierarchical architecture is more effective than LSTM's sequential processing in extracting the critical spatial features from the input data for this specific task. Furthermore, CNN's accuracy and comprehensive evaluation metrics surpass those of all shallow learning models, confirming its more advanced capability in transient stability assessment. In comparison, the Graph Neural Network (GNN) and Transformer models, as representative methods from 2023-2025, also demonstrate competitive performance with accuracy rates of 97.10% and 96.85% respectively. However, the proposed CNN-based approach outperforms both GNN and Transformer, highlighting its superiority in handling spatiotemporal trajectories of power systems. GNN's graph-based structure may not fully capture the temporal dynamics of generator swings, while Transformer's self-attention mechanism could be less efficient for local feature extraction compared to CNN's convolutional layers. This contrast underscores the importance of architecture optimization for transient stability assessment tasks.

To evaluate the efficacy of the proposed transient stability information matrix construction method in enhancing the prediction accuracy of the refined margin networks, tests were performed on both the improved stability and instability margin prediction networks. These networks utilized the arrangement method introduced earlier. Based on an established empirical formula, we set the number of neurons in the hidden layer of both BP prediction networks to 13. The prediction accuracy of these enhanced networks under the different arrangement methods is quantitatively compared in Figure 14 and Figure 15.

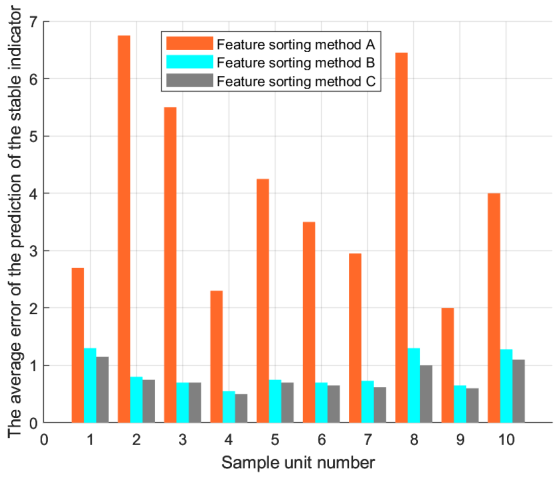

Figure 14. Average Prediction Error of the Stability Margin Index (TSI)

As shown in Figure 14, the mean error of stability margin prediction using Feature Arrangement Method A is over twice that of the other two arrangement methods. In contrast, stability margin prediction using Feature Arrangement Method C (sorted by disturbance severity) achieves mean errors within similar accuracy ranges compared to Method B (unsorted by disturbance severity), yet still exhibits moderate improvements in assessment accuracy.

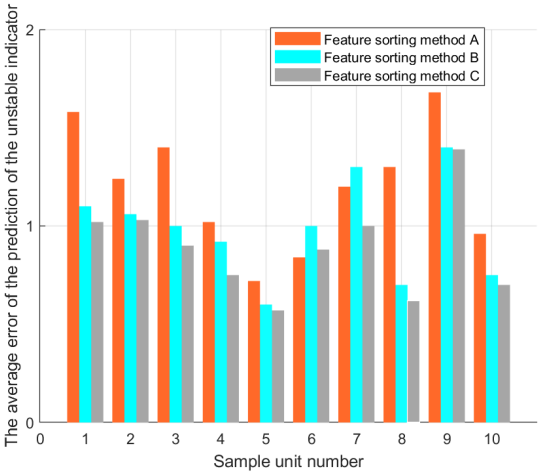

Figure 15. The average error of the forecast of the unstable indicator

As shown in Figure 15, the mean error of instability margin prediction using Feature Arrangement Method C (sorted by disturbance severity) is smaller than that of the other two arrangement methods. In summary, the feature arrangement method proposed in this paper is equally applicable to both system stability margin prediction and instability margin prediction, while enhancing prediction accuracy. To validate the advantages of the improved margin prediction network, the prediction capabilities of the improved margin prediction network and BP network are compared. Using the previously defined input feature arrangement method and optimal network parameters, the prediction accuracy of stability indices and instability indices is evaluated. The BP network is configured with 400 input neurons, 10 output neurons, and 20 hidden layer neurons set via empirical formula. The mean errors of predicted indices are statistically analyzed. The detailed results for stability and instability metrics are provided in Table 5 and Table 6, respectively.

Table 5. The average error of the stability metric predicted by the two networks

AE Network model	Improve the stability network	BP Network	AE Network model	Improve the stability network	BP Network
Unit 1	1.1500	3.7928	Unit 6	0.7528	3.8167
Unit 2	0.9138	6.5211	Unit 7	0.6890	3.3897
Unit 3	0.7825	5.0898	Unit 8	0.9172	7.2497
Unit 4	0.5913	3.3076	Unit 9	0.6826	2.8263
Unit 5	0.8610	4.3933	Unit 10	1.1324	5.5112

Table 6. The average error of the instability metric predicted by the two networks

AE Network model	Improving the instability network	BP Network	AE Network model	Improving the instability network	BP Network
Unit 1	1.0250	1.5662	Unit 6	0.8841	0.9203
Unit 2	1.0377	1.3232	Unit 7	1.0080	1.2097
Unit 3	0.9975	1.4617	Unit 8	0.6989	1.5079
Unit 4	0.7390	1.1579	Unit 9	1.3887	1.7264
Unit 5	0.5617	0.8105	Unit 10	0.7363	1.1876

A sensitivity analysis was conducted to evaluate the impact of the number of hidden layer neurons in the BP network on prediction accuracy. The number of neurons was varied within a range of 5 to 30, and the corresponding prediction performance was measured using the mean absolute error (MAE) for both the stability margin index (TSI) and instability index (UI). Results indicated that the prediction error initially decreased as the number of neurons increased, reaching an optimum around 13 neurons, beyond which further increases led to marginal improvements or slight degradation due to overfitting. This analysis confirms that the selected hidden layer size strikes a balance between model complexity and generalization capability, ensuring robust margin prediction while maintaining computational efficiency.

The comparative results presented in the tables indicate that the proposed improved stability and instability margin networks both achieve a lower mean prediction error than the standard BP network. This performance superiority validates the enhancement offered by the CNN-based architecture. The key advantage stems from the CNN's feature extraction layers, which can automatically uncover implicit, high-level features within the data—a capability that surpasses the limited representational power of the shallow BP network structure. Consequently, the improved margin networks demonstrate higher prediction accuracy.

Robustness Validation under Noise and Synchronization Errors: Gaussian white noise is injected into input trajectories with signal-to-noise ratios (SNR)

ranging from 20 dB to 5 dB. The CNN model maintains an accuracy above 96% and a false positive rate below 4% across all noise levels, outperforming SVM and ANN. The max-pooling layers and input standardization effectively suppress noise interference. For synchronization bias, simulated time delays (0.01–0.05 s) are applied to PMU data by shifting trajectory sampling points. The model exhibits minimal performance degradation (accuracy drop < 2%) due to the trajectory sorting strategy, which enhances spatial correlation among critical generators. Under combined non-ideal conditions, the comprehensive metric η remains above 95%, demonstrating strong robustness for real-world applications.

The high accuracy and low prediction errors achieved across diverse operating scenarios within the IEEE 39-bus system indicate the model's excellent intra-system generalization capability. This success is attributed to the physically-informed trajectory sorting strategy and the optimized CNN architecture, which effectively capture the underlying swing dynamics. However, the model's inter-system generalization—i.e., its ability to maintain performance when applied to unseen power systems with different network structures—constitutes an essential area for further investigation. The proposed feature engineering, particularly the generator sorting based on relative kinetic energy, is grounded in universal transient stability principles. Nevertheless, its optimality and the model's parameter sensitivity across heterogeneous systems warrant future research.

4.3 Validation under Diverse Fault Types and High Renewable Energy Penetration

To further validate the robustness and generalizability of the proposed method under more realistic and challenging grid conditions, additional tests were conducted involving diverse fault types and a high penetration scenario of renewable energy. The IEEE 39-bus system was modified by replacing the conventional synchronous generator at bus 36 with a wind farm equivalent, representing a 30% renewable energy penetration by capacity. Simulations were performed for three distinct fault types: a three-phase short-circuit fault (the base case), a single-line-to-ground (SLG) fault, and a line-to-line (LL) fault, all applied at the midpoint of line 34 with a duration of 0.2 seconds. For each fault type, 10,000 samples were generated under varied operating conditions, following the same data splitting procedure (9,000 for training, 1,200 for testing).

The assessment accuracy and stability margin prediction errors for the proposed CNN model across these scenarios are summarized in Table 7. Under the single-line-to-ground and line-to-line faults, the model maintained high accuracy levels of 98.35% and 98.20%, respectively. These values are only marginally lower than the 98.42% accuracy achieved for the three-phase fault, demonstrating the model's strong adaptability to different fault characteristics. The mean prediction errors for the Transient Stability Index (TSI) remained below 3.2% for both stable and unstable samples across all fault types, indicating reliable quantitative assessment capability. In the high renewable energy penetration scenario, the system's reduced inertia introduces more complex transient dynamics. Despite this increased complexity, the proposed model achieved an accuracy of 97.85%, with a TSI prediction error of 3.45%. This slight performance degradation compared to the traditional scenario (TSI error < 3%) is attributed to the increased volatility and noise in the generator trajectories caused by the wind power injection. However, the model's trajectory sorting strategy, which prioritizes generators with high relative kinetic energy, effectively mitigates these challenges by focusing feature extraction on the most critically disturbed units. The results confirm that the proposed method exhibits satisfactory robustness and generalization performance under a wider range of power system disturbances and modern grid architectures.

Table 7. Performance evaluation under diverse fault types and high renewable energy penetration

Scenario	Fault type	Assessment accuracy (%)	TSI Prediction Error (Mean AE, %)	Comprehensive Metric η (%)
Traditional Generation1	Three-Phase Short-Circuit	98.42	2.98	98.57
Traditional Generation	Single-Line-to-Ground (SLG)	98.35	3.10	98.43
Traditional Generation	Line-to-Line (LL)	98.20	3.15	98.28
High Renewable Penetration (30%)	Three-Phase Short-Circuit	97.85	3.15	97.92

5. Conclusions

Transient stability is a cornerstone of power system security. Nevertheless, the large-scale in-tegration of renewable energy and the development of complex hybrid AC/DC grids have markedly elevated the risk of transient instability. The occurrence of such instability can trigger a cascade of failures, resulting in widespread blackouts with severe socioeconomic consequences. Hence, the de-velopment of rapid and accurate assessment methods is critically important.

This paper proposes an improved CNN-based transient stability assessment method for power systems. By fusing early fault dynamics with deep learning techniques, it achieves dual objectives: transient stability state discrimination and stability margin prediction. To address the insufficient extraction of high-dimensional trajectory features in traditional methods, we innovatively construct a transient stability information matrix that

accounts for generator disturbance severity. This reorganizes rotor angular velocity and power angle trajectories into a 2D input format based on unit dynamic characteristics, enhancing the model's ability to characterize key generator responses and reducing misclassification risks. In network architecture design, guided by the dimension-matching principle of convolution kernels and pooling windows, we propose a comprehensive metric-driven network parameter optimization strategy. This constructs a deep feature extraction model with alternating convolutional-pooling layers, significantly improving adaptability to noise and imbalanced data sce-narios. To further quantify stability margins, a composite framework combining a CNN classifier and an improved CNN-BP prediction network is designed. This hierarchical assessment mechanism balances discrimination accuracy and margin computation efficiency. Simulations demonstrate that the method rapidly assesses stability states using short-term disturbance trajectories and excels in stabil-ity margin prediction, offering a novel technical pathway for online grid security analysis. Future research could integrate real-time wide-area measurement data to extend applications to complex grids with high renewable energy penetration, advancing the development of intelligent grid dynamic security frameworks.

It is important to note that the experimental validation in this study was conducted exclusively on the IEEE 39-bus system under a wide range of operating conditions. While the proposed method demonstrates strong generalization capabilities within this specific system, its performance on power systems with fundamentally different scales, topologies, and dynamic characteristics (e.g., the IEEE 118-bus system or practical regional grids) remains to be verified. Future work will prioritize cross-system validation to comprehensively evaluate the model's robustness and general applicability, which is a critical step towards practical deployment.

Acknowledgements

This research was funded by Basic Research Program of Jiangsu(BK20251833).

References

[1] Venkatasubramanian, V.; Liu, X.; Liu, G.P.; Zhang, Q.; Sherwood, M. Overview of Wide-Area Stability Monitoring Algorithms in Power Systems using Synchrophasors. In *Proceedings of the American Control Conference (ACC),* San Francisco, CA, USA, 29 June–1 July 2011; pp. 4172–4176.

[2] Hou, H.; Tang, A.H.; Fang, H.L.; Yang, X.L.; Dong, Z.Y. Electric Power Network Fractal and Its Relationship with Power System Fault. *Tehnicki Vjesnik-Technical Gazette* 2015, *22*, 623–628.

[3] Karacelebi, M.; Cremer, J.L. Online Neural Dynamics Forecasting for Power System Security. Int. J. Electr. Power Energy Syst. 2025, 167, 110566.

[4] Han, Z.X.; Wu, G.Y. Power System Analysis; Zhejiang University Press: Hangzhou, China, 1997.

[5] Poursaeed, A.H.; Namdari, F. Online Transient Stability Assessment Implementing the Weighted Least-Square Support Vector Machine with the Consideration of Protection Relays. Prot. Control Mod. Power Syst. 2025, 10, 1–17.

[6] Su, F.; Zhang, B.; Yang, S. A Novel Termination Algorithm of Time-Domain Simulation for Power System Transient Stability Analysis Based on Phase-Plane Trajectory Geometrical Characteristic. In *Proceedings of the 5th International Conference on Electric Utility Deregulation and Restructuring and Power Technologies (DRPT)*, Changsha, China, 2015; pp. 1422–1426.

[7] Wang D, Rueda Torres JL, Rakhshani E and van der Meijden M. MVMO-Based Identification of Key Input Variables and Design of Decision Trees for Transient Stability Assessment in Power Systems With High Penetration Levels of Wind Power. Front. Energy Res. 2020, 8, 41.

[8] Shrivastava, D.R., Siddiqui, S.A. & Verma, K. New Data Driven Scheme for Real-Time Power System Transient Stability Assessment. J. Electr. Eng. Technol. 2023, 18, 1745–1756.

[9] Lee, H.; Kim, J.; Park, J.H.; Chung, S.-H. Power System Transient Stability Assessment Using Convolutional Neural Network and Saliency Map. Energies 2023, 16, 7743.

[10] Singh, M., Chauhan, S. Transient Stability Assessment of Power Systems Integrating Wind Energy Utilizing Detailed Models and a Hybrid Ensemble Technique. Arab J Sci Eng, 2025, 50, 17723 – 17741.

[11] Sarajcev, P.; Kunac, A.; Petrovic, G.; Despalatovic, M. Artificial Intelligence Techniques for Power System Transient Stability Assessment. Energies 2022, 15, 507.

[12] H. Shin, J. Jung, S. Oh, K. Hur, K. Iba and B. Lee. Evaluating the Influence of Momentary Cessation Mode in Inverter-Based Distributed Generators on Power System Transient Stability. IEEE Transactions on Power Systems. 2020, vol. 35, no. 2, pp. 1618-1626.

[13] S. M. Al Araifi, M. S. E. Moursi and S. M. Djouadi. Individual Functions Method for Power System Transient Stability Assessment. IEEE Transactions on Power Systems, 2020, vol. 35, no. 2, pp. 1264-1273.

[14] Koichiro Shimizu, Atsushi Ishigame. Transient stability assessment application using post-disturbance voltage fluctuations in a multi-machine power system. International Journal of Electrical Power & Energy Systems. 2022, 139, 107987.

[15] Dmitry Efimov, Sergey Stashkevich. Coherence indicators of generators for express assessment of electric power system transient stability. E3S Web of Conf. 2023, 384, 01012.

[16] Shahriyari, M.; Khoshkhoo, H.; Guerrero, J.M. A Novel Fast Transient Stability Assessment of Power Systems Using Fault-On Trajectory. IEEE Syst. J. 2022, 16, 4334 – 4344.

[17] Tina, G.M.; Maione, G.; Licciardello, S. Evaluation of Technical Solutions to Improve Transient Stability in Power Systems with Wind Power Generation. Energies 2022, 15, 7055.

[18] Badrudeen, T.U.; Nwulu, N.I.; Gbadamosi, S.L. Neural Network Based Approach for Steady-State Stability Assessment of Power Systems. Sustainability 2023, 15, 1667.

[19] Zhang, S.; Zhu, Z.; Li, Y. A Critical Review of Data-Driven Transient Stability Assessment of Power Systems:

Principles, Prospects and Challenges. Energies 2021, 14, 7238.
[20] Zhou, B.; Xu, Y.; Sun, X.; Ye, X.; Wang, Y.; Dai, H.; Gao, S. Multiple Stability Margin Indexes-Oriented Online Risk Evaluation and Adjustment of Power System Based on Digital Twin. Energies 2025, 18, 4804.
[21] Yao, J., Zhao, H., Hu, Y. et al. Physics-Informed LSTM for Real-Time Voltage Stability Assessment of Power Systems with High Renewable Energy Integration. Smart Grids and Energy 10, 80 (2025).
[22] X. Yang.; Y. Dong, J. Wang and C. Wang, Transient Voltage Prediction Method Based on Spatial-Temporal Graph Convolutional Network, *2022 9th International Forum on Electrical Engineering and Automation* , Zhuhai, China, 2022, 1174-1178,.
[23] Cheng, S.; Yu, Z.H.; Liu, Y.; Zuo, X.W. Power System Transient Stability Assessment Based on the Multiple Paralleled Convolutional Neural Network and Gated Recurrent Unit. *Prot. Control Mod. Power Syst.* 2022, *7*, 39.
[24] Xie, T.; Hu, Z.H.; Zhang, W.D.; Chen, H.T. Fault Diagnosis for Multi-Phase Inverters: A Telescoping Modulus Approach with Convolutional Neural Networks. *IEEE Trans. Circuits Syst.* 2024, *71*, 4371–4375.
[25] Lee, H.; Kim, J.; Park, J.H.; Chung, S.H. Power System Transient Stability Assessment Using Convolutional Neural Network and Saliency Map. *Energies* 2023, *16*, 7743.
[26] Q. Zhang et al. Adaptive Identification of Power System Operational States Based on Spatio-Temporal Dynamic Graph Neural Networks, *2024 IEEE 4th International Conference on Electronic Technology, Communication and Information*, Changchun, China, 2024, 910-916.
[27] Zhang, Z.; Liu, Y.H. Stochastic Stability Analysis of Power Systems Under Gauss Small Random Excitation. In *Proceedings of the 35th Chinese Control Conference (CCC)*, Chengdu, China, 27–29 July 2016; pp. 1039–1044.
[28] B. R. Sri.; T. S. Balakrishnan. Classification of Pests in Agricultural Farms Using Convolutional Neural Network Compared to Artificial Neural Network, *2024 15th International Conference on Computing Communication and Networking Technologies*, Kamand, India, 2024, 1-4.
[29] Wang, H.M.; Li, Z.J. A Review of Power System Transient Stability Analysis and Assessment. In *Proceedings of the 2019 IEEE Prognostics and System Health Management Conference (PHM-Qingdao)*, Qingdao, China, 25–27 October 2019.